



Macrocrack extension by connecting statistically distributed microcracks

SULIN ZHANG and WEI YANG

Department of Engineering Mechanics, Tsinghua University, Beijing 100084, China

Received 24 September 1997; accepted in revised form 6 April 1998

Abstract. The present paper explores the extension of a macrocrack by connecting statistically distributed microcracks. Two issues are discussed: (1) how long a semi-infinite crack can extend by connecting collinear microcracks of equal length but distributed ligament sizes; (2) how far the crack tip can shift vertically from the original crack extension line by connecting randomly positioned and oriented microcracks. Statistical analysis is employed to calculate the expected crack extension length and the vertical shift of the crack tip. The implication of the present study for the problem of a macrocrack linking to a parallel fault is addressed.

Key words: Fracture, macrocrack–microcrack interaction, expected extension length, vertical shift, statistical analysis.

1. Introduction

The existence of many microcracks has been recognized as a major strength degradation mechanism in brittle materials. Some researchers attributed the damage evolution toward fracture to the reduction of effective elastic constants. This perception has encouraged research into the estimation of the effective stiffness, with approaches ranging from the Mori–Tanaka method (1973), the self-consistent method of Budiansky and O’Connell (1976) to the generalized self-consistent method of Christensen and Lo (1979). Nevertheless, the effective elastic property is not a reliable indicator of damage prediction for brittle materials (Wu and Chudnovsky, 1990; Kachanov, 1992). The fracture related parameters such as the stress intensity factors (SIF) are sensitive to the local microcrack geometry, while the effective elastic properties, as volume average quantities, are not.

The local interaction should be taken into account in describing the fracture of brittle materials, as exemplified in many macrocrack–microcracks interaction analyses (Kachanov, 1990, 1992). The immense computations render a direct numerical evaluation of macrocrack–microcracks interaction impractical. Since the scatter in fracture related properties is inherent to brittle materials, a statistical approach would be a natural way to deal with the problem.

The macrocrack–microcracks interaction has been extensively discussed in the literature; see Kachanov et al. (1990). However, the complete fracture process due to the macrocrack connecting to microcracks has hardly been addressed. A comprehensive review on the background of this area can be found in Kachanov (1992), where some basic concepts are clarified. Coalescence between collinear microcracks in brittle materials toward fracture was investigated recently by Zhang et al. (1998), with an emphasis on the strong interactions among the microcracks.

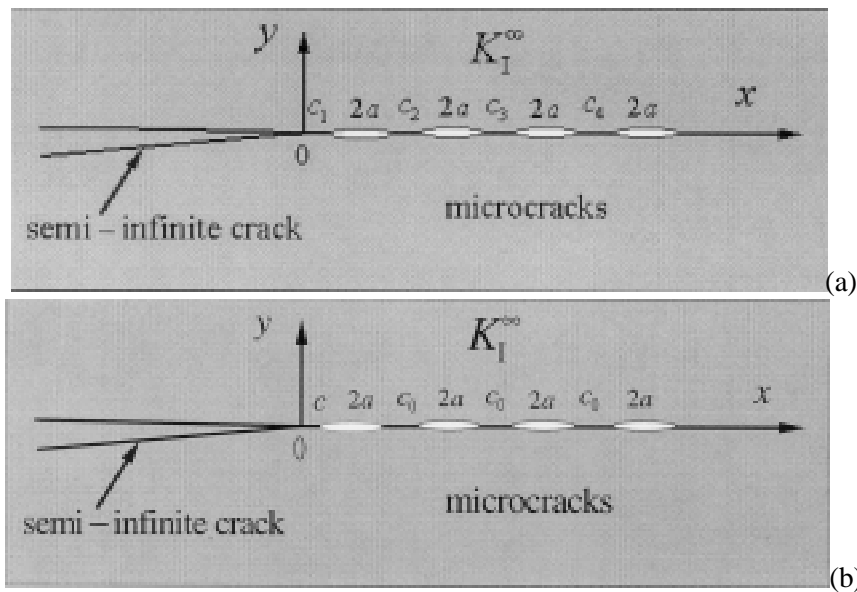


Figure 1. Configurations of collinear microcracks lying ahead of a semi-infinite crack. (a) Array of microcracks with arbitrary lengths and ligament sizes; (b) array of microcracks with remote periodical configuration.

The present work analyzes the extension of a macrocrack by connecting microcracks on its way. For brevity, we assume the material to be isotropic and linear elastic, and the macrocrack to be driven by remote mode I loading. Since the deviation of crack path from its original direction is of interest here, issues such as material anisotropy, mixed mode loading and T -stress influence are certainly of relevance. Be this as it may, we confine the present analysis to the simplest case, and focus on the demonstration that the statistical nature of the microcrack distribution can itself generate a fluctuating crack path, even in the absence of mixed mode loading and T -stress. The readers should bear in mind that further inclusion of a mode II component and a tensile T -stress will capitalize the crack path deviation. The material's anisotropy will twist the crack path further by offering different elastic response and different fracture toughness in various directions.

As a geometrical simplification of the problem, the lengths of the microcracks and the ligaments are assumed to be much smaller than the macrocrack length, with the latter being regarded as semi-infinite and extending self-similarly. This simplification may overestimate the extension of the macrocrack, but will retain the statistical nature of the problem. As will be shown below, the simulation by self-similar crack propagation enables us to quantify the macrocrack propagation by linking microcracks for many steps.

To get analytical results, we cannot start from arbitrarily positioned and oriented microcracks, along with completely unknown statistical features. Instead, we simulate the general situation in three steps:

- (i) For the interaction among cracks, we consider a collinear array of cracks with random positions, as shown in Figure 1(a). The analysis then highlights the local interaction between the macrocrack and the nearest microcrack, and replaces the other microcracks by a periodic array, as shown in Figure 1 (b).
- (ii) Next we consider arbitrary orientations and lateral positions of the nearest microcrack, and search for their influence on the vertical deviation of the microcrack. Similar to the

computational damage cell model, only the damage cell directly ahead of the main crack is of relevance to the crack path, while the microcrack in the cell may have a different orientation. The weakening by the other microcracks, if treated as a degradation of the Young's modulus, would have no effect on the SIF of the macrocrack. By linking those microcracks one at a time along probabilistic tilting angles, one finds the probabilistic vertical shift. The expected vertical shift is shown to be proportional to the square root of the linking step n .

- (iii) Then we combine the two analyses. The first calculation delivers the linking step n under a prescribed remote SIF, and the substitution of that n value into the second calculation leads to an estimate of the vertical shift. It is an approximate scheme, but it does reveal the qualitative aspect of the vertical shift.

The above approach requires the examination of two cases in detail. The first case concerns the expected extension of the macrocrack by linking an array of collinear microcracks. The second case treats the more general case of randomly positioned and oriented microcracks, with attention focused on the vertical shift of the macrocrack from its original path. Both cases involve the estimation of the interacting stress intensity factor at the tip of the macrocrack and a statistical analysis to predict the macrocrack extension.

The next section recapitulates the available results for the stress intensity factors at the semi-infinite crack tip under the above mentioned microcrack configurations. Section 3 conducts a statistical evaluation of the expected extension of the macrocrack under a prescribed remote stress intensity factor. Section 4 estimates the vertical shift of the semi-infinite crack by linking randomly positioned and oriented microcracks. The last section combines the two analyses to predict the crack path deviation under a prescribed mode I load.

2. Stress intensity factor at a semi-infinite crack tip

2.1. A COLLINEAR MICROCRACK ARRAY AHEAD OF THE SEMI-INFINITE CRACK

Consider the problem of an array of collinear microcracks ahead of a semi-infinite crack in an otherwise infinite plane, as depicted in Figure 1a. The semi-infinite crack occupies the negative x -axis and the array of *microcracks* is situated at $x_k^l < x < x_k^r$ ($k = 1, 2, 3 \dots$), where the superscripts 'l' (or 'r') refers to the left (or the right) tip of the microcrack. The configuration is subjected to a remote stress intensity factor K_I^∞ . The complex potential formulation of linear plane elasticity is employed (Muskhelishvili, 1953)

$$\begin{aligned} \sigma_{11} + \sigma_{22} &= 4\phi'(z), \\ \sigma_{22} - \sigma_{11} + 2i\sigma_{12} &= 2(\bar{z}\phi''(z) + \psi'(z)), \\ u_1 + iu_2 &= \frac{1+\nu}{E}(\kappa\phi(z) - z\overline{\phi'(z)} - \overline{\psi(z)}) \end{aligned} \tag{1}$$

where $\kappa = 3 - 4\nu$ for the plane strain case, $\kappa = (3 - \nu)/(1 + \nu)$ for the plane stress case, and E and ν are the Young's modulus and the Poisson's ratio, respectively. The symmetry of the problem admits a single potential representation, for example, by $\phi(z)$, for all field quantities.

For the configuration considered, Rubinstein (1985) introduced the following stress function that satisfies all the boundary conditions

$$\phi'(z) = \frac{K_I(\infty)}{2\sqrt{2\pi z}} \frac{\prod_{k=1}^N (\lambda_k - z)}{\sqrt{\prod_{k=1}^N (x_k^l - z)(x_k^r - z)}}, \quad (2)$$

where N is the number of microcracks, and λ_k ($k = 1, 2, 3, \dots, N$) are real constants which can be determined by the condition of single valued displacements

$$\int_{x_k^l}^{x_k^r} \text{Im } \phi'(x) dx = 0, \quad k = 1, 2, \dots, N. \quad (3)$$

The stress intensity factor at the tip of the semi-infinite crack is

$$\frac{K_I}{K_I^\infty} = \frac{\prod_{k=1}^N \lambda_k}{\sqrt{\prod_{k=1}^N x_k^l x_k^r}}. \quad (4)$$

For the special microcrack configuration delineated in Figure 1(b), the microcracks have the same half-length $a = a_0$, and the ligaments between the neighboring microcracks assume the same value of c_0 . However, the first ligament, namely the ligament between the macrocrack and the nearest microcrack, may have a different value of c . Then the right hand side of (4) depends only on the dimensionless groups c/d_0 and a_0/d_0 , with $d_0 = 2a_0 + c_0$ being the distance between the centers of two neighboring microcracks, and a_0/d_0 signifying the microcrack density. Thus, one may tabulate the SIF at the macrocrack tip ($x = 0$) as follows

$$K_I = K_I^\infty Y\left(\frac{c}{d_0}, \frac{a_0}{d_0}\right) \quad (5)$$

where Y is a dimensionless shape function. Details of the calculation of function Y can be found in the work of Rubinstein (1985).

2.2. AN ARBITRARY MICROCRACK NEAR THE SEMI-INFINITE CRACK

We next evaluate the interacting SIF of the semi-infinite crack by an arbitrarily positioned and oriented microcrack, loaded by a mode I stress intensity factor K_I^∞ , as shown in Figure 2. The microcrack has a length $2a$ and an orientation θ . The line from the semi-infinite crack tip to the center of microcrack has a length d and spans an angle φ from the extension line of the macrocrack. Rubinstein (1986) studied this problem using complex stress potentials, and a singular integral equation was formulated. The derivation leading to the singular integral equation is facilitated by an interacting stress function of a single dislocation with the arbitrarily positioned and oriented microcrack. Taking the semi-infinite crack as an array of many

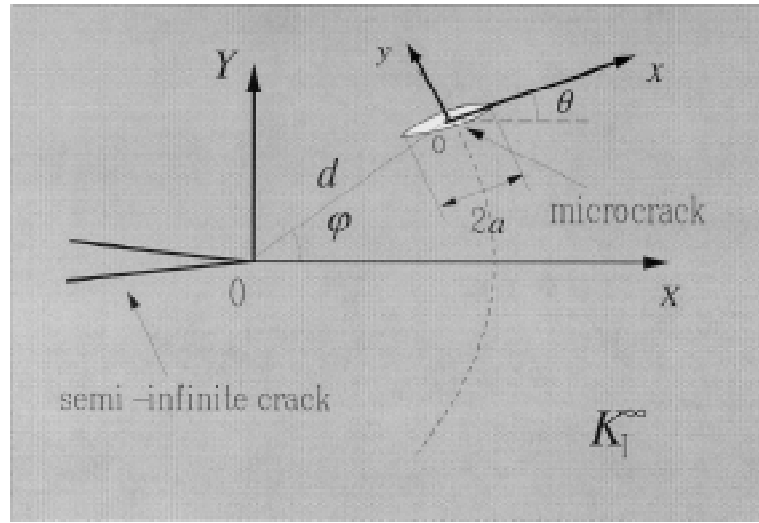


Figure 2. Configuration of an arbitrarily positioned and oriented microcrack near a semi-infinite crack.

dislocations, one can write down the complex potential in terms of a superposition integral describing the interaction of the microcrack with the semi-infinite crack

$$\begin{aligned}\phi'(z) &= \int_{-\infty}^0 \left[\frac{E'b(\xi)}{8\pi i(z-\xi)} + \phi'_0(b, z, \xi) \right] d\xi + \phi'_{00}(z), \\ \psi'(z) &= \int_{-\infty}^0 \left[-\frac{E'}{8\pi i} \left(\frac{\bar{b}(\xi)}{(z-\xi)} - \frac{\xi b(\xi)}{(z-\xi)^2} \right) + \psi'_0(b, z, \xi) \right] d\xi + \psi'_{00}(z)\end{aligned}\quad (6)$$

where $E' = E/(1 - \nu^2)$ for the plane strain case and $E' = E$ for the plane stress case. In each equation above, the first term in the integrand represents the dislocation self-field, and the second term represents the interaction of the microcrack with a dislocation increment $b(\xi) d\xi$ positioned at ξ . The last term represents the field induced by the microcrack alone.

The integral equation, which defines the dislocation density $b(\xi)$, can be derived from the traction free condition along the semi-infinite crack. A numerical scheme featuring the Gauss–Chebyshev quadrature can solve the integral equation. Details of this integral equation, as well as the estimation of the stress intensity factors, were provided by Rubinstein (1986). The interaction of the microcrack gives the coexistence of K_I and K_{II} at the semi-infinite crack tip; they have the following form

$$K_{I,II} = K_I^\infty F_{I,II}(a/d, \varphi, \theta), \quad (7)$$

where a/d signifies the density of microcracks. F_I and F_{II} are dimensionless shape functions for mode I and mode II, respectively. For a tilted extension of the macrocrack, the energy release rate for crack tilting at an acute angle φ is (see Cotterell and Rice, 1980)

$$\begin{aligned}G &= \frac{K_I^{\infty 2}}{E'} \tilde{G}(a/d, \varphi, \theta) \\ &= \frac{K_I^{\infty 2}}{E'} \cos^2 \frac{1}{2} \varphi \{ \cos^2 \frac{1}{2} \varphi F_I^2 + (1 + 3 \sin^2 \frac{1}{2} \varphi) F_{II}^2 - 2 \sin \varphi F_I F_{II} \}.\end{aligned}\quad (8)$$

The authors have repeated the solution scheme of Rubinstein (1986) to get the F_I and F_{II} functions in (7), and to evaluate G from (8). Note that (8) gives the energy release rate for the macrocrack which starts to tilt toward (but yet to link to) the microcrack oriented at an acute angle φ . The numerical calculation reveals that the energy release rate of the semi-infinite crack decreases as the angle φ increases. In a fixed tilting direction φ , the orientation θ of the microcrack also effects the energy release rate (through the expressions in (7)).

A semi-infinite crack would link to a microcrack if the resulting energy release rate reaches a critical value

$$\tilde{G}(a/d, \varphi, \theta) = E'G_C/K_I^{\infty 2} \quad (9)$$

where G_C is the critical energy release rate (or the fracture toughness) of the material. Under prescribed values of a/d and φ , \tilde{G} would maximize at a certain microcrack orientation θ . This maximum value can be calculated by

$$\tilde{G}_{\max}(a/d, \varphi) = \max_{\forall \theta} \tilde{G}(a/d, \varphi, \theta). \quad (10)$$

Given a prescribed value of a/d , a critical value of φ , denoted by φ_0 , for a fixed value of $E'G_C/K_I^{\infty 2}$ is obtained

$$\tilde{G}_{\max}(a/d, \varphi_0) = E'G_C/K_I^{\infty 2}. \quad (11)$$

A microcrack with angle $|\varphi| > \varphi_0$ cannot link to the macrocrack, regardless of its orientation angle. For the case of $|\varphi| < \varphi_0$, a linking range $\theta_1 \leq \theta \leq \theta_2$ of microcrack orientations can be identified. For prescribed values of a/d and φ , the bounding orientations θ_1 and θ_2 are determined by

$$\tilde{G}(a/d, \theta_{1,2}, \varphi) = E'G_C/K_I^{\infty 2}. \quad (12)$$

The above discussions on the possible linking ranges have implicitly taken into account the effect of microcrack shielding (for large φ angles). The microcrack orientations that have a significant shielding effect have already been ruled out from the possible linking range.

3. Statistical extension of a semi-infinite crack

Attention is now focused on the statistical process for the extension of a semi-infinite crack by coalescing to collinear microcracks, as depicted in Figure 1a. The half length of the microcracks is denoted by a , and the ligament size between the semi-infinite crack and the nearest microcrack or between two neighboring microcracks is denoted by c . For simplicity, we consider the case of equal microcrack length but distributed ligament size. The statistical distribution of c is described by a density function $f(c)$, which is properly normalized and has a lower limit of c_- . Since the ligament sizes are statistical variables, the solution of the stress intensity factor at the macrocrack tip is burdensome. Note that the size of the first ligament dominates the SIF at the macrocrack tip. As depicted in Figure 1b, we approximate the sizes of the other ligaments by the expected value $c_0 = \int_{c_-}^{\infty} cf(c) dc$, then the microcrack array ahead of the macrocrack becomes almost periodic, except that the first ligament size, c , is still a random variable and different from the expected value c_0 in general.

The microcrack configuration in Figure 1b was thoroughly discussed by Rubinstein (1985), and the solution was presented earlier in (5). His study indicated that the normalized stress intensity factor at the main crack tip increases as the microcrack density a_0/d_0 increases, and as the first ligament size c/d_0 decreases. The monotonic variation of Y with respect to the first ligament size enables us to define a threshold value of K_I^∞ , denoted by K_{th}^∞ , such that

$$K_{th}^\infty = K_{IC} / Y \left(\frac{c_-}{d_0}, \frac{a_0}{d_0} \right) \tag{13}$$

where K_{IC} is the matrix fracture toughness. Under a given remote stress intensity factor, a critical ligament size c^* is defined by

$$Y \left(\frac{c^*}{d_0}, \frac{a_0}{d_0} \right) = K_{IC} / K_I^\infty. \tag{14}$$

From the above equation, $c^* < c_-$ when $K_I^\infty < K_{th}^\infty$, and the semi-infinite crack remains intact; when $K_I^\infty > K_{th}^\infty$, c^* would exceed c_- , and the first ligaments of sizes smaller than c^* would break. The probability for the first extension of the semi-infinite crack is

$$p_1 = \int_{c_-}^{c^*} f(c) dc. \tag{15}$$

By the first connection, the average extension length of the macrocrack can be written as

$$L_1 = \frac{1}{p_1} \int_{c_-}^{c^*} cf(c) dc + 2a_0. \tag{16}$$

The subsequent connections follow similar procedures. We change the size of the next ligament to a random variable c and repeat and almost similar analysis. The difference between the first connection and the others lies in the reduced number of ligaments whose sizes fall in the range of $[c_-, c^*]$. Suppose that there are N microcracks ahead of the main crack, then only Np_1 ligaments of them are breakable (after rounding off to an integer). For the k th step, the number of the remaining ligaments becomes $N - k + 1$, while the number of the breakable ligaments reduces to $Np_1 - k + 1$. The probability of the k th connection and the extension of the main crack for the k th step become

$$p_k = \frac{Np_1 - k + 1}{N - k + 1}, \quad L_k = L_1. \tag{17}$$

Under a prescribed stress intensity factor, the expected extension length of the semi-infinite crack is

$$L_{\text{expect}} = \sum_{k=1}^{Np_1} \left(\prod_{j=1}^k p_j \right) L_k. \tag{18}$$

The above equation indicates that the expected crack extension depends not only on the remote stress intensity factor, but also on the number of the microcracks, since p_k is a monotonically decreasing function of N , from (17). The expected crack extension increases as the remote

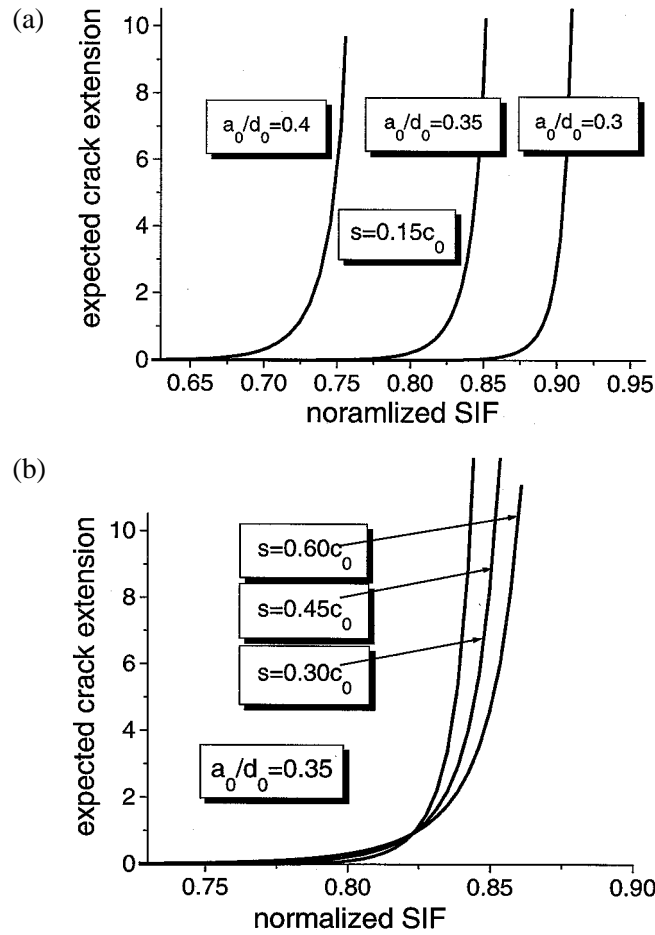


Figure 3. Expected extension length of a semi-infinite crack vs the normalized stress intensity factor. (a) $s = 0.15c_0$; (b) $a_0/d_0 = 0.35$.

intensity factor or the number of the microcracks increases. The relationship between the expected extension and the number of the microcracks indicates a scale dependency of brittle materials.

For the case of infinitely many microcracks, p_k approaches p_1 . Therefore, each step exactly repeats the procedure of the first step. The expected extension of the main crack becomes

$$L_{\text{expect}} = \sum_{k=1}^{\infty} p_1^k L_1 = \frac{p_1 L_1}{1 - p_1}. \quad (19)$$

We see that the present statistical analysis delivers a closed form estimate for the expected extension of macrocracks under a prescribed mode I stress intensity factor. Equation (19) indicates that the expected extension of the main crack diminishes if p_1 approaches zero; and becomes infinite if p_1 approaches one.

Figure 3 plots the expected extension of the semi-infinite crack versus the normalized remote stress intensity factors K_I^∞/K_{IC} . We prescribe $f(c)$ by a normal distribution which peaks at c_0 . Figure 3(a) is plotted under a standard deviation of $s = 0.15c_0$, with various curves corresponding to different microcrack densities of 0.3, 0.35 and 0.4. The expected

extension of the semi-infinite crack slowly rises as the normalized SIF exceeds the threshold value K_{th}^∞/K_{IC} , then undergoes a transition, and finally approaches the vertical asymptote for the catastrophic crack extension. As the microcrack density increases, the transition of the expected crack extension starts at a smaller K_I^∞/K_{IC} value. In Figure 3(b) the microcrack density is fixed at 0.35, with various curves corresponding to different s/c_0 values of 0.3, 0.45 and 0.6. The expected extension of the semi-infinite crack increases as the standard deviation increases when the remote stress intensity factor is low, but decreases as the standard deviation increases when the remote stress intensity factor is high. This variation can be explained as follows: when the standard deviation is high, there are more ligaments of both small and large sizes. Under a low remote stress factor, the probability of the semi-infinite crack connecting to microcracks increases since there are more breakable small ligaments; when the remote intensity factor is high, on the other hand, there are more unbreakable ligaments and they retard the crack extension.

The present statistical analysis can be adopted for the case that microcracks are created by the high stress field near the macrocrack tip. Assuming the newly created microcrack is collinear with the macrocracks and has a fixed half-length a_0 and a random ligament c . Following Rubinstein (1985), the stress intensity factor at the macrocrack tip is

$$K_I = K_I^\infty \sqrt{\frac{2a_0 + c}{c}} \frac{E\left(\frac{2a_0}{2a_0 + c}\right)}{K\left(\frac{2a_0}{2a_0 + c}\right)} \tag{5'}$$

where $K(m)$ and $E(m)$ are complete elliptical integrals of the first and second type, respectively. Determination of the critical size of ligament c^* is reduced from (14) to

$$\sqrt{\frac{2a_0 + c^*}{c^*}} \frac{E\left(\frac{2a_0}{2a_0 + c^*}\right)}{K\left(\frac{2a_0}{2a_0 + c^*}\right)} = K_{IC}/K_I^\infty. \tag{14'}$$

4. Vertical shift of the semi-infinite crack tip

Consider microcracks positioned and oriented ahead of a semi-infinite crack. The configuration is loaded remotely by an applied stress intensity factor K_I^∞ . We want to emphasize that the random nature of the microcrack orientations provokes the zigzag in the cracking path. The fluctuating vertical shift intensifies as more microcracks are connected, even though the remote loading and the statistical distribution of the microcracks are symmetric with respect to the x -axis. Suppose the macrocracks grows a long distance. We want to estimate the expected vertical shift of the crack tip from the original crack extension line. In geological structures, a long crack may connect microcracks under geological stress and deviate from its original path. The present case refers to the linkage of two noncoplanar macroscopic defects driven by the normal loading in a brittle material microcracks. Linkage of two geological faults under remote shear loading can be analyzed by this approach, with slight modification. The vertical shift means that it is possible that two parallel geological faults may join, and has significance in analyzing catastrophic geological ruptures, such as earthquakes.

We first propose a simple model to describe the vertical shift of a semi-infinite crack. The extension of the semi-infinite crack is accomplished via step-by-step connections between the semi-infinite crack and the neighboring microcracks. In each step, the linking process is dominated by the energy release rate for the macrocrack to extend toward the microcrack, while the effect of the other microcracks is secondary. The simplified configuration in Figure 2 can be interpreted as follows. On one hand, one can treat the effect of other cracks (assuming completely random orientation) as an isotropic weakening of the elastic modulus, which bears no effect on the stress intensity factor near the tip of the macrocrack. On the other hand, the macrocrack-microcrack interaction shown in Figure 2 resembles the exact situation for the case that the microcrack is newly created by the high stress field, accompanied by the propagation of the macrocrack.

According to this model, the process shown in Figure 2 repeats itself. The SIF for the macrocrack and the energy release rate criteria are discussed in Section 2.2, through Expressions (7), (8) and (9). Each step causes a small vertical shift. After n steps of microcrack connections, those vertical shifts may sum to a sizable deviation from the original crack extension line. The distribution of the microcracks is simulated as follows. The center of the microcrack nearest to the semi-infinite crack appears with equal probability $1/2\pi$ along a circle centered at the tip of the macrocrack. The radius of the circle is denoted by d , and remains constant in all connecting steps. All microcracks are assumed to have an equal length $2a$. Suppose that macrocrack-microcrack linking does occur; the linking probability of the semi-infinite crack towards a microcrack in the direction φ is denoted by p_φ , which is calculated by

$$p_\varphi = \int_{\theta_1(\varphi)}^{\theta_2(\varphi)} f(\theta) d\theta \bigg/ \int_{-\varphi_0}^{+\varphi_0} \int_{\theta_1(\varphi)}^{\theta_2(\varphi)} f(\theta) d\theta d\varphi. \quad (20)$$

In the above equation, $f(\theta)$ ($-\pi/2 \leq \theta \leq \pi/2$) is a normalized microcrack orientation distribution function. Under a given remote stress intensity factor, φ_0 is furnished by (11) and θ_1 (or θ_2) by (12) for a given $\varphi \leq \varphi_0$. Any microcrack with its orientation outside the range of $[\theta_1(\varphi), \theta_2(\varphi)]$ could not connect to the semi-infinite crack extending in the direction φ . The standard deviation of the tilting of the semi-infinite crack is

$$s^2 = \int_{-\varphi_0}^{+\varphi_0} (\varphi - \bar{\varphi})^2 p_\varphi d\varphi \quad (21)$$

where $\bar{\varphi}$ is the expected value of φ

$$\bar{\varphi} = \int_{-\varphi_0}^{+\varphi_0} \varphi p_\varphi d\varphi. \quad (22)$$

The symmetry of the problem leaves the estimation of the probability p_φ only on the upper half plane $\varphi > 0$, and the expected angle $\bar{\varphi}$ becomes zero. A threshold value of the remote stress, denoted by K_{th}^∞ , satisfies the following equation

$$K_{\text{th}}^\infty = \frac{\sqrt{EG_c}}{F_1(a/d, 0, 0)}. \quad (23)$$

The semi-infinite crack could not connect to any arbitrary oriented microcracks if K_1^∞ is less than K_{th}^∞ . Otherwise, a linking probability exists. As a demonstrative example, we evaluate

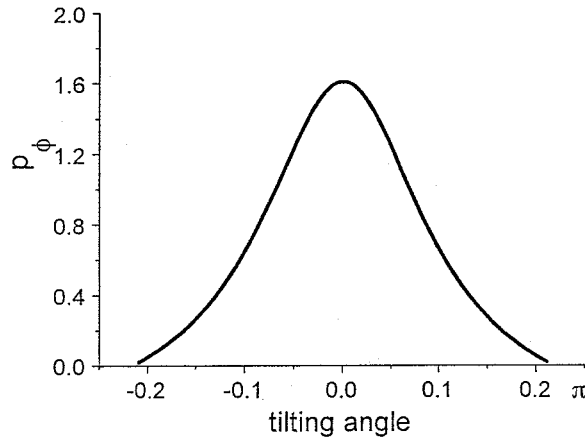


Figure 4. Linking probability versus microcrack orientation.

the distribution p_φ at $K_I^\infty = 1.2K_{th}^\infty$ under uniform orientation distribution of microcracks ($f(\theta) = 1/\pi$). The calculated distribution of p_φ is depicted in Figure 4. This distribution approximately resembles a normal distribution. Data fitting according to (21) gives a standard deviation of 0.25 for the probability distribution p_φ in Figure 4. As shown in the figure, the probability for crack tilting is symmetric with respect to the x -axis, and favors a tilting by small angles. A tilting angle beyond 0.22π is prohibited by the crack shielding effect.

We next discuss the vertical shift after the semi-infinite crack extends n steps. Denote the tilting direction for the i th step by φ_i , then the vertical shift h_i in that step is given by

$$h_i = d \times \sin \varphi_i \approx d \times \varphi_i. \tag{24}$$

Here d is a constant. The approximation in the last step holds when the extension direction φ_i is much smaller than $\pi/2$. In this case, φ_i and h_i has the same probability distribution, denoted by $p_i(h_i)$. The total vertical shift after n steps is denoted by H_n , and is evaluated by

$$H_n = \sum_{i=1}^n h_i. \tag{25}$$

Expression (25) resembles a random walk solution. Random walking, in a strict sense, refers to equal possibilities to walk into any direction. Nevertheless, the walker will not stay at the starting point, but drift farther and farther away. The problem here is a modified random walk problem, since the probability of the tilting angle (calculated and plotted in Figure 4) is not uniform, but is concentrated along the crack extension line.

Denote the probability for the semi-infinite crack tip to get to the height H after n connections by $p(H)$; on then has

$$p(H) = \int_{-\infty}^{+\infty} \left\{ \int_{-\infty}^{+\infty} \dots \int_{-\infty}^{+\infty} \prod_{i=1}^{n-1} p_i(h_i) p_n(H - H_{n-1}) dh_i \right\} dh_n. \tag{26}$$

The convolution integral in (26) suggest a solution by Fourier transform

$$\tilde{p}(\eta) = \int_{-\infty}^{+\infty} \exp(-i\eta H) p(H) dH. \tag{27}$$

Substituting (26) into (27), one arrives at

$$\tilde{p}(\eta) = \prod_{i=1}^n \tilde{p}_i(\eta) \quad (28)$$

where the Fourier transforms of $p_i(h_i)$, $i = 1, 2, \dots, n$, are denoted by $\tilde{p}_i(\eta)$. For the case of a semi-infinite crack, each extension step of the macrocrack is self-similar, thus

$$p_1(h_1) = p_i(h_i), \quad i = 1, 2, \dots, n \quad (29)$$

which reduces (28) to

$$\tilde{p}(\eta) = [\tilde{p}_1(\eta)]^n. \quad (30)$$

As remarked in the calculation leading to Figure 4, the probability distribution of p_φ can be approximated by a normal distribution. The approximation (24) henceforth implies that the probability distribution of $p_i(h_i)$ for the vertical shift of each linking step can be represented by a normal distribution

$$p_i(h) = \frac{1}{\sqrt{2\pi}s} \exp\left(-\frac{h^2}{2s^2}\right), \quad i = 1, 2, \dots, n \quad (31)$$

where the standard deviation s can be estimated by data fitting. For example, s equals approximately $0.25d$ for the case of $K_1^\infty = 1.2K_{th}^\infty$ under the approximation (24). The Fourier transform of (31) gives

$$\tilde{p}_i(\eta) = \frac{2}{\sqrt{2\pi}s} \int_0^{+\infty} \cos(\eta h) \exp\left(-\frac{h^2}{2s^2}\right) dh = \exp(-s^2\eta^2/2) \quad (32)$$

and consequently from (30) one has

$$\tilde{p}(\eta) = \exp(-ns^2\eta^2/2). \quad (33)$$

The inverse transformation gives

$$p(H) = \frac{1}{\pi} \int_0^{+\infty} \cos(\eta H) \exp(-ns^2\eta^2/2) d\eta = \frac{1}{\sqrt{2\pi ns}} \exp\left(-\frac{H^2}{2ns^2}\right). \quad (34)$$

The above equation indicates that the vertical shift can be described by a normal distribution. The possible locations of the main crack are centered at $y = 0$, as indicated in (34), where $H = 0$ defines the mean value of the normal distribution of the vertical shift. However, (34) also indicates that the standard deviation, and consequently the vertical shift of the macrocrack tip, increase in proportion to the square root of the linking steps n as \sqrt{ns} .

5. Concluding remarks

The present paper explores two issues: the expected extension length and the expected vertical shift of a macrocrack by connecting nearby microcracks. Under a prescribed remote stress

intensity factor, it is revealed that the expected extension length depends not only on the microcrack density, but also on the fluctuation of the ligament sizes. The number of microcracks also plays a role on the expected extension of the macrocrack, giving rise to a scaling effect.

The other issue is related to the statistical analysis on the vertical shift of a semi-infinite crack. A scenario of macrocrack extension by linking arbitrarily positioned and oriented microcracks is proposed, and the linking probability to microcracks of different inclination angles is calculated. It is found the linking probability distribution resembles a normal distribution. Thus, a random walk scheme is adopted to predict the distribution of vertical shift after n steps of macrocrack-microcrack linkages. Statistical analysis indicates that the main crack has a vertical shift proportional to the square root of n .

Consider a macrocrack propagating in a microcrack-weakened geological structure. Suppose there is another major geological fault parallel to the macrocrack, and lying above or below by a vertical distance of H . Though we only work out the remote mode I loading here, it is believed that the present scheme may also be adopted for the remote mode II loading. The macrocrack extends a length d by connecting one nearby microcrack. The macrocrack will connect to the faulting, with disastrous consequence such as an earthquake, when

$$s\sqrt{nd} = H \quad (35)$$

where $nd = L_{\text{expect}}$ is the expected crack extension length as discussed in Section 3, and depends on the microcrack density, the ligament fluctuation, the number of microcracks, and the remote stress intensity factor. The standard deviation s increases as $K_I^\infty/K_{\text{th}}^\infty$ increases, as discussed in Section 4. These results, in combination with formula (35), provide a fairly complete description on the problem of a macrocrack connecting to a geological fault.

Acknowledgement

The authors thank the support by the National Science Foundation on this research project.

References

- Budiansky, B. and O'Connell, R.J. (1976). Elastic moduli of a crack solid. *International Journal of Solids and Structures* **12**, 81–97.
- Christensen, R.M. and Lo, K.H. (1979). Solutions for effective shear properties in three phase sphere and cylinder models. *Journal of the Mechanics and Physics of Solids* **27**, 315–330.
- Cotterell, B. and Rice, J.R. (1980). Slightly curved or kinked cracks. *International Journal of Fracture* **16**, 155–169.
- Kachanov, M. (1992). Effective elastic properties of cracked solids: Critical review of some basic concepts. *Applied Mechanics Review* **45**, 304–335.
- Kachanov, M., Montagut, E. and Laures, J.P. (1990). Mechanics of crack-microcrack interactions. *Mechanics of Materials* **10**, 59–71.
- Mori, T. and Tanaka, K. (1973). Average stress in matrix and average elastic energy of materials with misfitting inclusions. *Acta Metallurgica* **21**, 571–583.
- Muskhelishvili, H.N. (1953). *Some Basic Problems of the Mathematical Theory of Elasticity*, Noordhoff, Groningen.
- Rubinstein, A.A. (1985). Macrocrack interaction with semi-infinite microcrack array. *International Journal of Fracture* **27**, 113–119.
- Rubinstein, A.A. (1986). Macrocrack-microdefect-interaction. *Journal of Applied Mechanics* **53**, 505–511.
- Wu, S. and Chudnovsky, A. (1990). The effective elastic properties of a linear elastic solid with microcracks. *Engineering Fracture Mechanics* **37**, 653–659.
- Zhang, S., Yang, W. and Li, T. (1998). Statistical strength of brittle materials with strongly interacted collinear microcracks. *International Journal of Solids and Structures* **35**, 995–1008.